

# EVALUATION OF COMPLEX PERMITTIVITIES OF MULTILAYER DIELECTRIC SUBSTRATES AT MICROWAVE FREQUENCIES USING WAVEGUIDE MEASUREMENTS

R. L. Cravey<sup>1</sup>, M. D. Deshpande<sup>2</sup>, C. J. Reddy<sup>3</sup>, and P. I. Tiemsin<sup>1</sup>

(1) NASA Langley Research Center, Hampton, Virginia 23681

(2) ViGYAN Inc., Hampton, Virginia 23681

(3) Hampton University, Hampton, Virginia 23688

## ABSTRACT

The techniques that are presently available for the measurement of complex permittivities of dielectric substrates are only applicable to single layer substrates. This paper presents a new technique which uses the Finite Element Method (FEM) to estimate the complex permittivities of individual layers from the measurement of the S-parameters of a rectangular waveguide holding a multilayer dielectric substrate sample. In this method, a network analyzer is used to measure reflection and transmission coefficients of a rectangular waveguide loaded with a layered sample. Using FEM, the reflection and transmission coefficients are determined as a function of the complex permittivities of the multilayer substrate. Measured and calculated values of the reflection and transmission coefficients are then matched using the Newton-Raphson Method to estimate the complex permittivities of the layers of the sample.

Key words: *Permittivity Measurements, Finite Element Method*

## 1.0 INTRODUCTION

For the design of multilayer microwave integrated circuits it is necessary to know the complex permittivity of each individual layer of multilayer substrate material. Simple techniques to measure the dielectric constants of single layer substrate materials exist and are described in the literature [1] - [3]. These techniques involve fabrication of microstrip lines using the material under test as a substrate. In [4], the dielectric constants of substrates have been determined using a slotted waveguide into which the substrate samples are inserted. This technique, which uses measured S-parameters and the characteristic equation for the dominant mode in the guide to solve for the permittivity, requires the sample to be placed along the center of the waveguide. This technique is also valid for single layer substrates only.

In the method described in this paper, a waveguide is used as a sample holder for the substrates under test. The single or multilayered samples may be placed in any configuration in the guide. This technique is an extension of one described previously, in which the permittivity of a single layer sample was found by placing an arbitrarily shaped sample at any position in a

waveguide [5]. In the present technique, the reflection and transmission coefficients of the rectangular waveguide loaded with a layered sample are measured using a network analyzer. The problem geometry is then simulated with a computer-aided design program, which also produces a FEM grid with different material parameters assigned to each layer of the sample. The reflection and transmission coefficients as functions of permittivity are computed using FEM. The Newton-Raphson Method is used to determine the values of permittivity for which the measured and calculated reflection and transmission coefficients match.

Section 2.0 of this paper contains a discussion of the theory used to compute the reflection and transmission coefficients for given material parameters. Section 3.0 describes the technique used to obtain the measured values of the S-parameters. In Section 4.0, computation of sample permittivities from S-parameter data is explained. In Section 5.0, results are presented. Section 6.0 contains conclusions.

## 2.0 THEORY (DIRECT PROBLEM)

In this section FEM will be used to determine the reflection and transmission coefficients of a rectangular transmission line loaded with a multilayer dielectric material. Figure 1 shows a rectangular waveguide with a layered dielectric sample. It is assumed that the waveguide is excited by a dominant TE<sub>10</sub> mode from the left. The reflection coefficient is measured at the reference plane P<sub>1</sub>, and the transmission coefficient is measured at the reference plane P<sub>2</sub>, as shown in figure 1(a). For the purpose of analysis the problem is divided into three regions; Region I (z < 0), Region II (0 ≤ z ≤ L), and Region III (z > 0).

Using the waveguide vector modal functions, the transverse electromagnetic fields in the regions I and III are expressed as [6]

$$\begin{aligned} \vec{E}^I(x, y, z) &= \vec{e}_0(x, y) e^{-j\gamma_0^I z} \\ &+ \sum_{p=0}^{\infty} a_p \vec{e}_p(x, y) e^{j\gamma_p^I z} \end{aligned} \quad (1)$$

$$\begin{aligned} \vec{H}^I(x,y,z) &= \vec{h}_0(x,y) Y_0^I e^{-j\gamma_0^I z} \\ - \sum_{p=0} a_p \cdot \vec{h}_p(x,y) Y_p^I e^{j\gamma_p^I z} \end{aligned} \quad (2)$$

$$\vec{E}^{III}(x,y,z) = \sum_{p=0}^{\infty} c_p \cdot \vec{e}_p(x,y) e^{-j\gamma_p^{III} z} \quad (3)$$

$$\vec{H}^{III}(x,y,z) = \sum_{p=0} c_p \cdot \vec{h}_p(x,y) Y_p^{III} e^{-j\gamma_p^{III} z} \quad (4)$$

In deriving equations (1) - (4) it is assumed that only the dominant mode is incident on the interface  $P_1$ , the  $a_p$  are the amplitudes of reflected modes at the  $z = 0$  plane, and the  $c_p$  are the amplitudes of transmitted modes at the  $z = L$  plane.  $Y_p^I$  and  $\gamma_p^I$  appearing in equations (1) - (4) are the characteristic admittance and propagation constant for the  $p^{th}$  mode and are as defined in [6]. The unknown complex modal amplitudes  $a_p$  and  $c_p$  may be obtained in terms of the transverse electric field over the planes  $P_1$  and  $P_2$  as follows:

$$1 + a_0 = \iint_{S_1} \vec{E}|_{\text{over } S_1} \cdot \vec{e}_0 ds \quad (5)$$

$$a_p = \iint_{S_1} \vec{E}|_{\text{over } S_1} \cdot \vec{e}_p ds \quad (6)$$

$$c_p = \iint_{S_2} \vec{E}|_{\text{over } S_2} \cdot \vec{e}_p ds \quad (7)$$

where  $S_1$  and  $S_2$  are the surface areas over the planes  $P_1$  and  $P_2$ .

The electromagnetic field inside Region II is obtained using the FEM formulation [7]. The vector wave equation for the  $\vec{E}^{II}$  field is given by

$$\nabla \times \left( \frac{1}{\mu_r} \cdot \nabla \times \vec{E}^{II} \right) - (k_0^2 \epsilon_r) \vec{E}^{II} = 0 \quad (8)$$

Using the weak form of the vector wave equation and some mathematical manipulation the equation (8) may be written as

$$\begin{aligned} & \iiint_V \left( \nabla \times \vec{T} \cdot \left( \frac{1}{\mu_r} \cdot \nabla \times \vec{E}^{II} \right) - (k_0^2 \epsilon_r) \vec{E}^{II} \cdot \vec{T} \right) dv \\ &= 2 \left( \frac{j\omega\mu_0}{\mu_r} \right) \cdot Y_0^I \cdot \iint_{S_1} \vec{T} \cdot \vec{e}_0(x,y) ds \\ & - \left( \frac{j\omega\mu_0}{\mu_r} \right) \cdot \left( \sum_{p=0}^{\infty} Y_p^I \left( \iint_{S_1} \vec{T} \cdot \vec{e}_p(x,y) ds \right) \right) \times \\ & \left( \iint_{S_1} \vec{E}^{II}|_{\text{over } S_1} \cdot \vec{e}_p(x,y) ds \right) \\ & - \left( \frac{j\omega\mu_0}{\mu_r} \right) \cdot \left( \sum_{p=0}^{\infty} Y_p^{III} \left( \iint_{S_2} \vec{T} \cdot \vec{e}_p(x,y) ds \right) \right) \times \\ & \left( \iint_{S_2} \vec{E}^{II}|_{\text{over } S_2} \cdot \vec{e}_p(x,y) ds \right) \end{aligned} \quad (9)$$

In order to solve equation (9), the volume enclosed by Region II is discretized by using first-order tetrahedral elements [7]. The electric field in a single tetrahedron is represented as

$$\vec{E}^{II} = \sum_{m=1}^6 b_m \cdot \vec{W}_m \quad (10)$$

where  $b_m$ ,  $m=1, 2, 3, \dots, 6$  are the six complex amplitudes of electric field associated with the six edges of the tetra-

hedron, and  $\vec{W}_m(x, y, z)$  is the vector basis function associated with the  $m$ th edge of the tetrahedron. A detailed derivation for the expression for

$\vec{W}_m(x, y, z)$  is given in reference [7]. Substituting equation (10) into equation (9), integration over the volume of one tetrahedron results in the element matrix equation

$$[S_{el}] \cdot [b] = [v] \quad (11)$$

where the entries of the element matrices are given by

$$S_{el}(m, n) = \iiint_V \left( \nabla \times \vec{W}_n \cdot \frac{1}{\mu_r} \nabla \times \vec{W}_m - k_0^2 \epsilon_r \vec{W}_m \cdot \vec{W}_n \right) dv$$

$$+ \left( \frac{j\omega\mu_0}{\mu_r} \right) \sum_{p=0}^{\infty} Y_p^I \left( \iint_{S_1} \vec{W}_n \cdot \vec{e}_p(x, y) ds \right) \times$$

$$\left( \iint_{S_1} \vec{W}_m \cdot \vec{e}_p(x, y) ds \right)$$

$$+ \left( \frac{j\omega\mu_0}{\mu_r} \right) \sum_{p=0}^{\infty} Y_p^{III} \left( \iint_{S_2} \vec{W}_n \cdot \vec{e}_p(x, y) ds \right) \times$$

$$\left( \iint_{S_2} \vec{W}_m \cdot \vec{e}_p(x, y) ds \right) \quad (12)$$

$$v(n) = 2 \left( \frac{j\omega\mu_0}{\mu_r} \right) \cdot Y_0^I \cdot \iint_{S_1} \vec{W}_n \cdot \vec{e}_0(x, y) ds \quad (13)$$

These element matrices can be assembled over all the tetrahedral elements in the Region II to obtain a global matrix equation

$$[S] \cdot [b] = [v] \quad (14)$$

The solution vector  $[b]$  of the matrix equation (14) is then used to determine the reflection coefficient at the reference plane  $P_1$  as

$$a_0 = \iint_{S_1} \vec{E}|_{\text{over } S_1} \cdot \vec{e}_0 ds - 1 \quad (15)$$

$$c_0 = \iint_{S_2} \vec{E}|_{\text{over } S_2} \cdot \vec{e}_0 ds \quad (16)$$

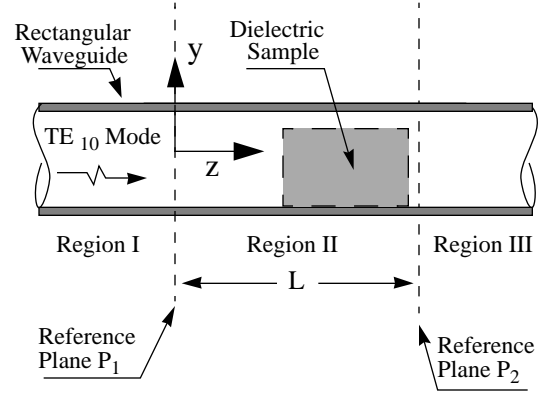


**Figure 1(a).** Longitudinal view of rectangular waveguide loaded with layered sample

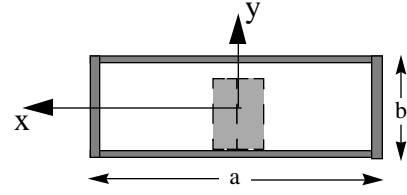


**Figure 1(b).** Cross sectional view of rectangular waveguide loaded with layered sample

**Figure 1.** Geometry of rectangular waveguide excited by  $TE_{10}$  mode

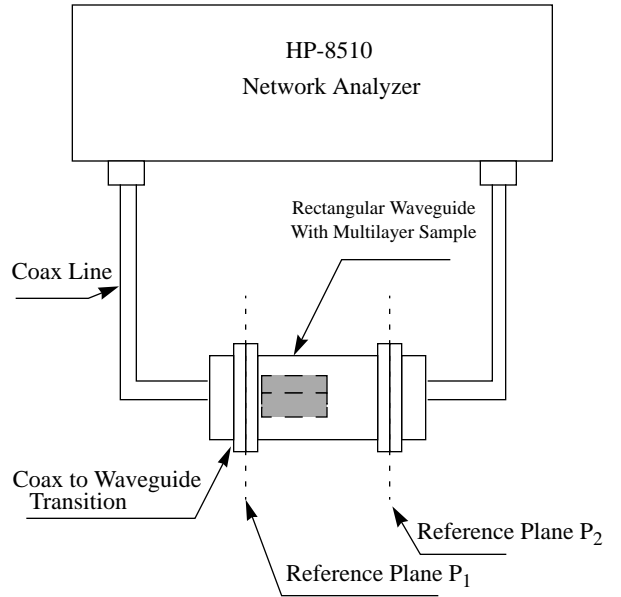


**Figure 2.** Rectangular waveguide measurement system

### 3.0 MEASUREMENT SETUP

The rectangular waveguide measurement system to measure the reflection coefficient is shown in figure 2. Before the measurement, a full two-port calibration using a standard waveguide calibration kit is done at the reference planes P<sub>1</sub> and P<sub>2</sub>. The reflection and transmission coefficients  $a_0'$  and  $c_0'$  of the rectangular waveguide with a layered sample piece are then measured as functions of frequency. If the sample piece occupied the entire cross section of the waveguide and was a single layer, an algorithm which uses the Nicholson-Ross Technique [8-9] could be used to determine the complex permittivity of the sample. However, the algorithm which is based on the Nicholson-Ross Technique cannot be used when the sample piece occupies only part of the cross section of rectangular waveguide, or for layered samples. When the dielectric sample is of arbitrary shape or layered the procedure described in next section is used

### 4.0 INVERSE PROBLEM

This section presents the computation of the complex dielectric constant of a given sample piece from the measurement of the reflection and transmission coefficients. From the given geometry of the sample and its position in rectangular waveguide the reflection coefficient  $a_0(\epsilon'_{r1}, \epsilon''_{r1}, \epsilon'_{r2}, \epsilon''_{r2})$  and the transmission coefficient  $c_0(\epsilon'_{r1}, \epsilon''_{r1}, \epsilon'_{r2}, \epsilon''_{r2})$  are calculated using the FEM for assumed values of  $(\epsilon'_{r1}, \epsilon''_{r1})$  and  $(\epsilon'_{r2}, \epsilon''_{r2})$ . If  $a_0'$  and  $c_0'$  are the measured reflection and transmission coefficients then the error in calculated values of reflection and transmission coefficients are  $a_0(\epsilon'_{r1}, \epsilon''_{r1}, \epsilon'_{r2}, \epsilon''_{r2}) - a_0'$  and  $c_0(\epsilon'_{r1}, \epsilon''_{r1}, \epsilon'_{r2}, \epsilon''_{r2}) - c_0'$ . Writing the errors in real and imaginary parts we get

$$f_1(\epsilon'_{r1}, \epsilon''_{r1}, \epsilon'_{r2}, \epsilon''_{r2}) = \text{real}(a_0 - a_0') \quad (17)$$

$$f_2(\epsilon'_{r1}, \epsilon''_{r1}, \epsilon'_{r2}, \epsilon''_{r2}) = \text{imag}(a_0 - a_0') \quad (18)$$

$$f_3(\epsilon'_{r1}, \epsilon''_{r1}, \epsilon'_{r2}, \epsilon''_{r2}) = \text{real}(c_0 - c_0') \quad (19)$$

$$f_4(\epsilon'_{r1}, \epsilon''_{r1}, \epsilon'_{r2}, \epsilon''_{r2}) = \text{imag}(c_0 - c_0') \quad (20)$$

If  $(\epsilon'_{r1}, \epsilon''_{r1}, \epsilon'_{r2}, \epsilon''_{r2})$  are incremented by small values to

$$(\epsilon'_{r1} + d\epsilon'_{r1}, \epsilon''_{r1} + d\epsilon''_{r1}, \epsilon'_{r2} + d\epsilon'_{r2}, \epsilon''_{r2} + d\epsilon''_{r2})$$

such that  $f_1(\cdot)$ ,  $f_2(\cdot)$ ,  $f_3(\cdot)$ , and  $f_4(\cdot)$  are

simultaneously zero then we can write following matrix equation [10]

$$\begin{bmatrix} \frac{\partial f_1}{\partial(d\epsilon'_{r1})} & \frac{\partial f_1}{\partial(d\epsilon''_{r1})} & \frac{\partial f_1}{\partial(d\epsilon'_{r2})} & \frac{\partial f_1}{\partial(d\epsilon''_{r2})} \\ \frac{\partial f_2}{\partial(d\epsilon'_{r1})} & \frac{\partial f_2}{\partial(d\epsilon''_{r1})} & \frac{\partial f_2}{\partial(d\epsilon'_{r2})} & \frac{\partial f_2}{\partial(d\epsilon''_{r2})} \\ \frac{\partial f_3}{\partial(d\epsilon'_{r1})} & \frac{\partial f_3}{\partial(d\epsilon''_{r1})} & \frac{\partial f_3}{\partial(d\epsilon'_{r2})} & \frac{\partial f_3}{\partial(d\epsilon''_{r2})} \\ \frac{\partial f_4}{\partial(d\epsilon'_{r1})} & \frac{\partial f_4}{\partial(d\epsilon''_{r1})} & \frac{\partial f_4}{\partial(d\epsilon'_{r2})} & \frac{\partial f_4}{\partial(d\epsilon''_{r2})} \end{bmatrix} \begin{bmatrix} d\epsilon'_{r1} \\ d\epsilon''_{r1} \\ d\epsilon'_{r2} \\ d\epsilon''_{r2} \end{bmatrix} = \begin{bmatrix} f_1(\cdot) \\ f_2(\cdot) \\ f_3(\cdot) \\ f_4(\cdot) \end{bmatrix} \quad (21)$$

From the solution of equation (21), new modified values of  $(\epsilon'_{r1}, \epsilon''_{r1}, \epsilon'_{r2}, \epsilon''_{r2})$  are obtained as

$$(\epsilon'_{r1})_{new} = \epsilon'_{r1} + d\epsilon'_{r1} \quad (22)$$

$$(\epsilon''_{r1})_{new} = \epsilon''_{r1} + d\epsilon''_{r1} \quad (23)$$

$$(\epsilon'_{r2})_{new} = \epsilon'_{r2} + d\epsilon'_{r2} \quad (24)$$

$$(\epsilon''_{r2})_{new} = \epsilon''_{r2} + d\epsilon''_{r2} \quad (25)$$

The reflection and transmission coefficients  $a_0(\cdot)$  and  $c_0(\cdot)$  with modified values of  $\epsilon'_{r1}, \epsilon''_{r1}, \epsilon'_{r2}, \epsilon''_{r2}$  are again calculated using the FEM procedure. With the new value of  $a_0(\cdot)$  and  $c_0(\cdot)$  computation through equations (17) - (25) are repeated. The above procedure is repeated till required convergence is obtained (i.e.  $d\epsilon'_{r1} \leq \Delta_1$ ,  $d\epsilon''_{r1} \leq \Delta_2$ ,  $d\epsilon'_{r2} \leq \Delta_3$

and  $d\epsilon''_{r2} \leq \Delta_4$  where the  $\Delta$ 's are preselected small quantities). The procedure described above will converge to the true value of complex permittivity if the first choice of  $(\epsilon'_{r1}, \epsilon''_{r1}, \epsilon'_{r2}, \epsilon''_{r2})$  is close to the true values of complex permittivities.

## 5.0 NUMERICAL RESULTS

For numerical results, samples made from RT/Duriod 5500 and Alumina substrate materials are considered. To validate the present method, first single layer substrate samples were constructed. An RT/Duriod sample of size (1.016 x 0.145 x 1.016 cm) was cut and placed in a x-band rectangular waveguide as shown in figure 3. Using a Hewlett-Packard 8510 network analyzer the reflection coefficient  $a_0'$  was measured over the x-band. From the measured and estimated values of reflection coefficients the complex permittivity was obtained and is presented in figure 3 along with the manufacturer's speci-

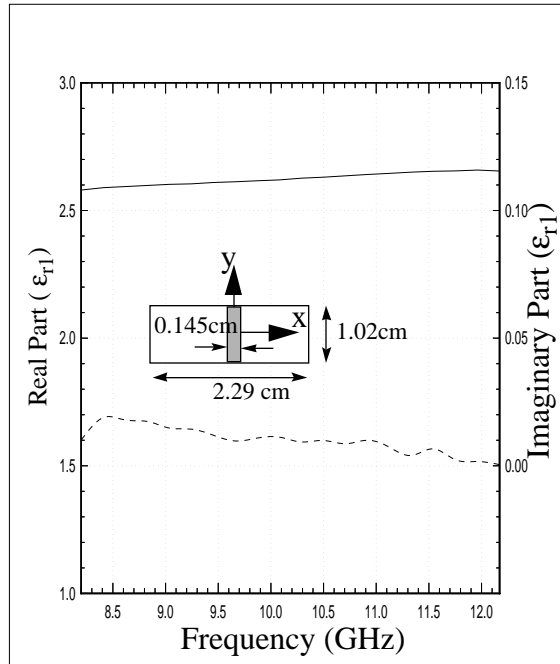


**Figure 3.** Real and imaginary parts of complex permittivity of RT/Duriod 5500 substrate over x-band. Manufacturer's specification:  $\epsilon_r' = 2.69$ ,  $\epsilon_r'' = 0.0054$

fied value.

For a sample constructed from Alumina substrate material, the sample size and its placement in the x-band rectangular waveguide was the same as given in figure 3. The estimate of its complex permittivity over the

x-band was determined using the procedure described here and is presented in figure 4 along with the manufacturer's specification. The estimate of complex permittivity for both samples agrees well with manufacturers specification.

To determine the permittivities of multilayer substrate, a sample made from RT/Duriod and Alumina substrates is placed in a waveguide as shown in figure 5. The reflection and transmission coefficients due to presence of such a sample in a x-band rectangular waveguide are then measured. From these measure-

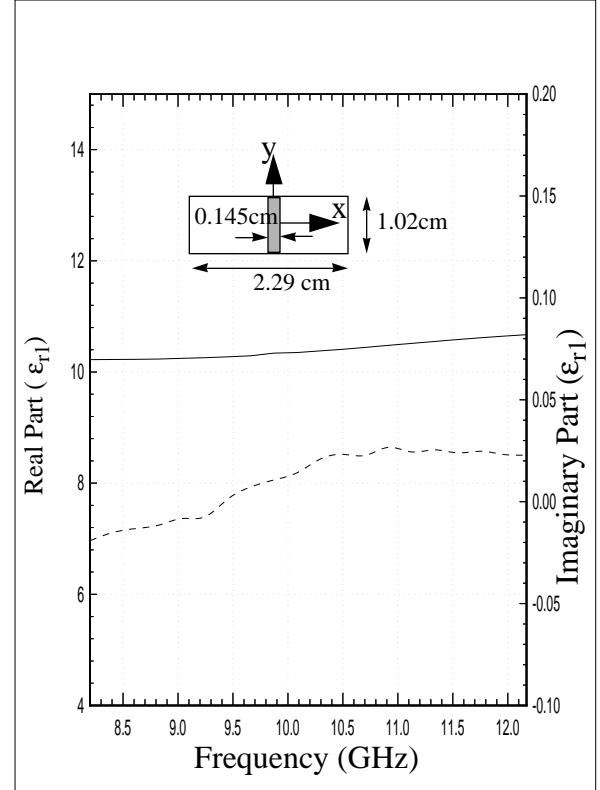


**Figure 4.** Real and imaginary parts of complex permittivity of Alumina substrate over x-band. Manufacturer's specification:  $\epsilon_r' \cong 10$ ,  $\epsilon_r'' \cong 0.001$

ments and following the procedure described in section 4.0 the dielectric constants of two layers are estimated. The results of these calculations will be presented at the conference.

## 6.0 CONCLUSIONS

An FEM procedure in conjunction with the Newton-Raphson Method has been presented to determine complex permittivity of a dielectric substrate material. The substrate sample is placed at the center of an X-band waveguide and reflection and transmission

coefficients are measured using a Hewlett-Packard 8510 Network Analyzer. For the same configuration of the x-band waveguide loaded with the sample piece, the reflection and transmission coefficients are calculated using the FEM as a function of complex dielectric constants. The Newton-Raphson Method is then used to determine the complex dielectric constant by matching the calculated values with the measured values. The computed values of complex permittivity of RT/Duriod and Alumina using the FEM method are in good agreement with the manufacturer's specifications.

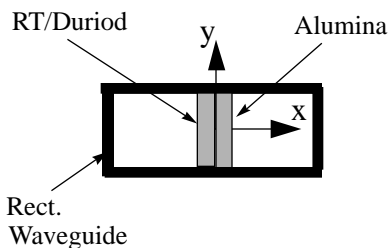


**Figure 5.** Geometry used for measurements of reflection and transmission coefficient due to two layers substrate.

## REFERENCES

- [1] Moon\_Que Lee & S. Nam, "An accurate broadband measurement of substrate dielectric constant," IEEE Microwave and Guided Wave Letters, Vol. 6, No. 4, pp. 168-170, April 1996.
- [2] N. K. Das, et al, "Two methods for the measurement of substrate dielectric constant," IEEE Trans. Microwave Theory Tech., Vol. MTT-35, No. 7, pp. 636-641, July 1987.
- [3] R. M. Pannell & B. W. Jervis, "Two simple methods for the measurement of the dielectric permittivity of low-loss microstrip substrates," IEEE Trans. Microwave Theory Tech., Vol. MTT-29, No. 4, pp. 383-386, April 1981.
- [4] R. A. York & R. C. Compton, "An automated method for dielectric constant measurements of microwave substrates," Microwave Journal, pp. 115-122, March 1990.
- [5] M. D. Deshpande, et al, "Measurement of complex permittivity of dielectric material at microwave frequency using waveguide measurements," 7th AMTA Symposium, Will-

iamsburg, VA., November 13-17, 1995.

- [6] R. F. Harrington, *Time-harmonic Electromagnetic Fields*, McGraw-Hill Book Company, New York, 1961.
- [7] C. J. Reddy, et al, "Finite element method for eigenvalue problems in electromagnetics," NASA Technical Paper 3485, December 1994.
- [8] Robin L. Cravey, et al, "Dielectric property measurements in the electromagnetic properties measurement laboratory", NASA Technical Memorandum 110147, April 1995.
- [9] "Dielectric material measurement forum," Hewlett Packard, 1993.
- [10] W. H. Press, et al, *Numerical recipes, The art of scientific computing (Fortran version)*, Cambridge University Press, Cambridge, 1989 (chap. 9).